Available online at www.sciencedirect.com
ScienceDirect
Journal of Molecular Spectroscopy 239 (2006) 94–100
Journal of MOLECULAR SPECTROSCOPY
www.elsevier.com/locate/jms

Microwave spectrum of the heterodimers: $CH_3OH–CO_2$ and $CH_3OH–H_2CO$

V.V. Ilyushin [a,*], F.J. Lovas [b], D.F. Plusquellic [b]

[a] Institute of Radio Astronomy of NASU, Chervonopraporna 4, 61002 Kharkov, Ukraine
[b] Optical Technology Division, National Institute of Standards and Technology, Gaithersburg, MD 20899-8441, USA

Received 15 May 2006; in revised form 31 May 2006
Available online 7 June 2006

Abstract

Molecular complexes, dimers and heterodimers often show interesting structures, large amplitude internal motions and orientations for reaction coordinates. These properties were the motivations for the current study of the rotational spectra of the heterodimers, $CH_3OH–CO_2$ and $CH_3OH–H_2CO$, in a pulsed nozzle Fourier-transform microwave (FTMW) spectrometer. In addition to studying the normal isotopic forms, several isotopologues containing ^{13}C or deuterium substituted atoms of each heterodimer were analyzed in order to obtain structural data of the complexes. All species showed splittings from internal rotation of the methyl group and splittings on the b-type transitions of the $CH_3OH–H_2CO$ species suggesting rotation of the H_2CO group between equivalent structural forms. Stark effect measurements on each of the parent species provided dipole moment components. Theoretical *ab initio* results are compared to the experimentally determined molecular parameters.

Keywords: Molecular complex; Dimer; Methanol–carbondioxide; Methanol–formaldehyde; Microwave spectrum; Structure; Dipole moment

1. Introduction

Rotational studies of molecular dimers and heterodimers have provided insights on reaction coordinates, e.g. $H_2CCH_2–O_3$ [1], large amplitude internal motions, e.g. $(CH_3OH)_2$ [2,3] and $(H_2CO)_2$ [4], and molecular structures of the lowest energy forms to verify the validity of theoretical calculations. The current study of the heterodimers $CH_3OH–CO_2$ and $CH_3OH–H_2CO$ was motivated by each of these objectives.

The methanol–carbon dioxide heterodimer has been the subject of laboratory and interstellar infrared investigation for its role in interstellar ice mantels [5–7]. While no high resolution experimental spectrum has been observed previously, theoretical calculations of the stable structural conformers and the infrared band associated with the CO_2 bend in the complex have been reported [8]. One of the objectives of the present study is to determine the most stable structural conformer for the heterodimer. Similarly, the $CH_3OH–H_2CO$ heterodimer has been the subject of theoretical study as a prototype for dihydrogen exchange between the alcohol and ketone structure [9], but no prior spectroscopic or structural study has been reported.

In the present paper we report the observation of both complexes by Fourier-transform microwave (FTMW) spectroscopy in the 8–26 GHz range. The rotation-centrifugal distortion-internal rotation molecular parameters have been determined for several isotopologues for each species enabling the determination of the conformations of each. Stark effect measurements provided the determination of the dipole moment components for the normal isotopic forms.

2. Experimental details

Spectral measurements were carried out with a Fabry–Perot cavity, Fourier-transform microwave spectrometer

* Corresponding author. Fax: +38 057 706 1415.
E-mail address: ilyushin@rian.kharkov.ua (V.V. Ilyushin).

0022-2852/$ - see front matter © 2006 Elsevier Inc. All rights reserved.
doi:10.1016/j.jms.2006.06.003

designed by Lovas and Suenram [10,11] of the Balle-Flygare type [12]. A new PC based system for timing and control of the mirrors, pulsed nozzle, microwave synthesizer, and signal processing has been incorporated and uses the FTMW++ software system designed by Grabow [13]. A pulsed solenoid valve was used to produce a supersonic molecular beam from a mixture of about one volume percent methanol and carbon dioxide entrained in argon (or neon) carrier gas at a total pressure of 100 kPa (1 atm) behind a 1 mm nozzle orifice and injected along the axis of the Fabry–Perot cavity and parallel to the microwave field. For the formaldehyde–methanol study, paraformaldehyde was placed in the reservoir of a heated pulsed nozzle and a one volume percent methanol sample entrained in argon (or neon) carrier gas served as backing gas. Molecular beam pulses with about 400 μs duration were employed with repetition rates up to 10 Hz. The molecular beam was polarized by a short microwave pulse when the microwave frequency was near-resonant ($\Delta v < 400$ kHz) with a rotational transition. The free induction decay signal from the cavity was digitized in 0.5 μs increments for 2048 channels. Typically, 50–100 pulses were signal averaged, after a background microwave pulse was subtracted from each signal pulse, to yield signal-to-noise ratios of 10 or more. The averaged data were Fourier transformed to obtain the amplitude spectrum in the frequency domain with a resolution element of 2 kHz/point. Molecular transitions observed as Doppler doublets had line widths of 5 kHz, and the frequency measurement uncertainties were estimated to be 4 kHz in most cases (type B with coverage factor $k = 2$ [14]), with the resolution element for the digitization time described above. Some transitions of the deuterated species exhibited partially resolved hyperfine structure, which caused larger uncertainties in the reported line centers.

3. Assignment and fit

Based on the B+C values for the CH_3OH–H_2CO and CH_3OH–CO_2 heterodimers from *ab initio* calculations [9] and general structural considerations, survey scans were made with the aim of finding *a*-type, *R*-branch transitions with low K_a values. These initial survey scans permitted the low K_a, a-type, R-branch transitions (both A and E species) to be readily assigned using features of JB95 [15]. Fig. 1 shows the survey scan over the $J = 3$–2 and $J = 4$–3 a-type transition regions for CH_3OH–CO_2. Note that clusters of lines from the methanol dimer overlap the methanol–carbon dioxide spectrum, but do not cause difficulty in the assignment. Fig. 2 shows a 1 GHz survey of the CH_3OH–H_2CO $J = 3$–2 *a*-type transition region. Both $(H_2CO)_2$ and Ar-CH_3OH were contaminants in this system, however their appearance did not complicate the assignment process. Further assignments were made in the usual bootstrap manner with fitting newly assigned transitions and obtaining improved predictions for unassigned transitions.

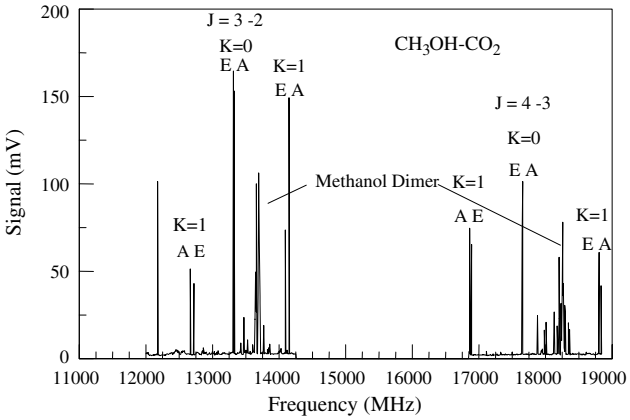

Fig. 1. Survey spectrum of CH_3OH–CO_2 showing the contamination from the methanol dimer.

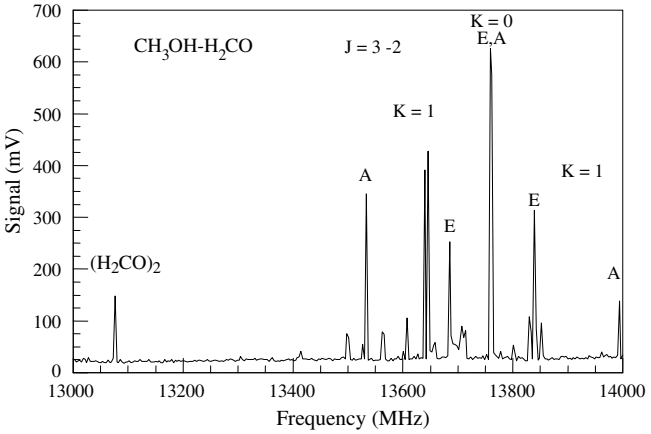

Fig. 2. Spectral scan of the $J = 3$–2 region of CH_3OH–H_2CO showing the A and E state splitting.

For the CH_3OH–H_2CO heterodimer, the *b*-type transitions (both A and E species) appeared as doublets due to a large amplitude motion of H_2CO unit that most likely corresponds to a 180° rotation of the H_2CO unit about its C_2 axis. The typical splitting observed for *b*-type transitions was about several tens of kHz, varying slightly depending on the type of the transition and deuteration of the formaldehyde unit. For the CH_3OH–H_2CO and CH_3OH–$H_2{}^{13}CO$ isotopologues, the weaker component of the doublets (one-third to one-half of the intensity of the stronger component) appeared at higher frequency, whereas for CH_3OH–D_2CO isotopologue, the weaker component was on the low frequency side of the doublet. In our fits, we used the upper frequency components of these *b*-type doublets for the lowest energy state which is consistent with the spin weights for the ground and excited states of 1:3 for H_2CO and 6:3 for D_2CO. For the CH_3OH–CO_2 heterodimer, there were no splittings observed for b-type transitions.

The assigned transitions for each isotopologue were fit using the so-called *rho*-axis method (RAM) Hamiltonian [16] that allows simultaneous fitting of transitions of A and E species. In the fits, we have used the uncertainties

Table 1
Torsion–rotation parameters for the CH_3OH–H_2CO, CH_3OH–$H_2{}^{13}CO$, and CH_3OH–D_2CO heterodimers in the ground torsional state[a]

Operator[b]	Parameter	CH_3OH–H_2CO	CH_3OH–$H_2{}^{13}CO$	CH_3OH–D_2CO
$1/2(1-\cos 3\gamma)$	V_3	240.53583(41)	240.31959(49)	239.20384(67)
P_γ^2	F	6.17[c]	6.16[c]	6.07[c]
$P_\gamma P_a$	ρ	0.16037949(94)	0.1588283(10)	0.1443300(14)
P_a^2	A	0.9100073(71)	0.8995958(93)	0.8134837(32)
P_b^2	B	0.0803578(90)	0.078802(10)	0.0763767(35)
P_c^2	C	0.074027(11)	0.072671(14)	0.07000566(55)
$\{P_a,P_b\}$	D_{ab}	−0.030986(19)	−0.029834(23)	−0.027525(25)
$-P^4$	D_J	$0.12267(16)\times10^{-6}$	$0.11884(15)\times10^{-6}$	$0.10773(17)\times10^{-6}$
$-P_a^4$	D_K	$-0.1039(66)\times10^{-3}$	$-0.1054(89)\times10^{-3}$	$0.05345(33)\times10^{-3}$
$-2P^2(P_b^2-P_c^2)$	δ_J	$0.680(14)\times10^{-8}$	$0.657(14)\times10^{-8}$	$0.661(13)\times10^{-8}$
$-\{P_a^2,(P_b^2-P_c^2)\}$	δ_K	$0.38(13)\times10^{-6}$	$0.35(12)\times10^{-6}$	$0.61(12)\times10^{-6}$
$P_\gamma^2P^2$	G_v	$-0.116(10)\times10^{-4}$	$-0.123(13)\times10^{-4}$	—
$(1-\cos 3\gamma)P^2$	F_v	$-0.172(28)\times10^{-3}$	$-0.189(35)\times10^{-3}$	$0.1319(20)\times10^{-3}$
$(1-\cos3\ \gamma)\{P_a,P_b\}$	d_{ab}	$-0.121(12)\times10^{-2}$	$-0.078(17)\times10^{-2}$	$-0.1306(83)\times10^{-2}$
Number of assigned lines		25A+31E	25A+30E	22A+31E
Root-mean square deviation/kHz		2.6	2.6	3.1

[a] All values are in cm^{-1}, except ρ, which is unitless. Type A uncertainties are shown as one standard deviation in the last two digits (coverage factor $k=1$) [14].
[b] $\{A,B\}=AB+BA$. The product of the operator and parameter from a given row gives the term actually used in the fit, except for F, ρ, and A which appear in the Hamiltonian in the form $F(P_\gamma-\rho P_a)^2+AP_a^2$.
[c] F parameter was fixed in the fits. See discussion in the text.

of 4 kHz for well resolved lines recorded with good signal-to-noise ratio and 10 kHz for some blended or weak lines. Table 1 presents the results of the fit for each isotopologue of CH_3OH–H_2CO giving the RAM Hamiltonian parameter values, total number of assigned transitions and root-mean-square (rms) deviation of the fit. Table 2 gives the same information for the isotopologues of CH_3OH–CO_2. It is seen from Tables 1 and 2 that for all isotopologues the rms deviations are less than 4 kHz uncertainty of the majority of the data. The measured frequencies of assigned transitions used in our fits, their uncertainties and observed minus calculated values from the final fits are available at ScienceDirect as Supplementary material for this article.

It should be noted that due to experimental conditions (supersonic expansion and frequency range from 7 to 26 GHz) we could measure only low J and low K_a transitions in the ground torsional state. For the CH_3OH–H_2CO heterodimer, we have assigned transitions with J

Table 2
Torsion-rotation parameters for the CH_3OH–CO_2, CH_3OH–$^{13}CO_2$, and CD_3OH–CO_2 heterodimers in the ground torsional state[a]

Operator[b]	Parameter	CH_3OH–CO_2	CH_3OH–$^{13}CO_2$	CD_3OH–CO_2
$1/2(1-\cos 3\gamma)$	V_3	174.7842(14)	174.8325(12)	157.934(12)
P_γ^2	F	5.45[c]	5.45[c]	2.83[c]
$P_\gamma P_a$	ρ	0.0419513(11)	0.04186181(98)	0.080916(48)
P_a^2	A	0.2993458(49)	0.2993685(47)	0.284248(82)
P_b^2	B	0.0982985(55)	0.0974728(52)	0.08767(15)
P_c^2	C	0.0659269(47)	0.0654754(46)	0.060870(21)
$\{P_a,P_b\}$	D_{ab}	−0.0591262(36)	−0.0589821(29)	−0.05292(20)
$-P^4$	D_J	$0.17202(20)\times10^{-6}$	$0.17059(20)\times10^{-6}$	$0.14712(21)\times10^{-6}$
$-P^2P_a^2$	D_{JK}	$0.133(16)\times10^{-6}$	$0.157(16)\times10^{-6}$	—
$-P_a^4$	D_K	$0.0991(14)\times10^{-5}$	$0.1017(11)\times10^{-5}$	$0.0966(12)\times10^{-5}$
$-2P^2(P_b^2-P_c^2)$	δ_J	$0.2846(16)\times10^{-7}$	$0.2827(20)\times10^{-7}$	$0.2445(16)\times10^{-7}$
$-\{P_a^2,(P_b^2-P_c^2)\}$	δ_K	—	—	$0.1248(35)\times10^{-6}$
$P_\gamma^2P^2$	G_v	$0.4033(50)\times10^{-4}$	$0.4008(49)\times10^{-4}$	$0.143(17)\times10^{-4}$
$(1-\cos 3\gamma)P^2$	F_v	$0.1576(10)\times10^{-2}$	$0.1566(10)\times10^{-2}$	$0.150(12)\times10^{-2}$
$P_\gamma^2P^2P_a^2$	k_{2J}	$-0.821(46)\times10^{-7}$	$-0.705(45)\times10^{-7}$	$-0.550(25)\times10^{-7}$
$(1-\cos 3\gamma)(P_b^2-P_c^2)$	c_2	$0.32853(78)\times10^{-3}$	$0.32674(48)\times10^{-3}$	$0.550(73)\times10^{-3}$
$(1-\cos 3\gamma)\{P_a^2,(P_b^2-P_c^2)\}$	c_{2K}	$-0.774(13)\times10^{-6}$	$-0.764(15)\times10^{-6}$	—
Number of assigned lines		32A + 42E	34A + 40E	37A + 37E
Root-mean square deviation/kHz		2.4	2.4	3.1

[a] All values are in cm^{-1}, except ρ, which is unitless. Type A uncertainties are shown as one standard deviation in the last two digits (coverage factor $k=1$) [14].
[b] $\{A,B\}=AB+BA$. The product of the operator and parameter from a given row gives the term actually used in the fit, except for F, ρ, and A which appear in the Hamiltonian in the form $F(P_\gamma-\rho P_a)^2+AP_a^2$.
[c] F parameter was fixed in the fits. See discussion in the text.

up to 9 and K_a up to 2 and for CH_3OH–CO_2 heterodimer, we have transitions with J up to 6 and K_a up to 4. This limited amount of data prevented the fitting of all zero order torsional parameters of the RAM Hamiltonian and, as usually done in such cases, we have fixed the F parameter in the fits. The F parameter was fixed at a value that corresponds to the moment of inertia of the methyl-top $I_\alpha = 3.21$ u Å^2 for the CH_3 group and 6.39 u Å^2 for the CD_3 group. These I_α values for the CH_3 and CD_3 groups used in our study were recalculated from the CH_3OH [17] and the CD_3OH [18] RAM Hamiltonian parameters, respectively. The I_α value was calculated using the equation for the F parameter given after equation (2–25) in the Lin and Swalen review on internal rotation [19].

The ratios of transitions to parameters in the fits vary from 3.9 to 1 in CH_3OH–$H_2{}^{13}CO$ to 5.3 to 1 in CD_3OH–CO_2, which are rather low. Although this is the usual situation for the investigation of complexes [20], one can expect that such low J and K_a transitions, sampling only the ground torsional state, should be fitted using zero order torsion and rotation parameters of the RAM Hamiltonian plus ordinary centrifugal distortion terms. Nevertheless, as seen from Tables 1 and 2, some higher order torsional parameters such as G_v, F_v, d_{ab}, k_{2J}, c_2, c_{2K} have been included in the model. The need for these parameters may be rationalized by the assumption that large fluctuational changes may occur in the symmetry plane of the heterodimer between methanol and its complex counterpart monomers (CO_2 and H_2CO in our case). Another possible explanation is that extra parameters in the model are needed to account of the influence of so-called libration motion of the methanol unit about its a inertial axis, which according to Fraser et al. [21] is responsible for dramatic lowering of the barrier. As seen from Tables 1 and 2 in our study, we also observed considerable lowering of the methyl-top internal rotation barrier to 240 cm^{-1} in the CH_3OH–H_2CO heterodimer and to 174 cm^{-1} in the CH_3OH–CO_2 heterodimer in comparison with 373 cm^{-1} in methanol itself.

4. Structural analysis

The structure was parameterized in the internal coordinates developed by Thompson, where each atom is specified by its orientation with respect to the last three specified atoms [22]. The coordinates consist of a bond length, a bond angle and a torsional angle. The structure fitting routine used was STRFTQ, written by Schwendeman [23] and modified by Lovas, which allows multiple isotopomers to be fit simultaneously.

In the structural fits, the planarity of the heavy atoms was assumed for both heterodimers. The planarity of the heavy atoms is evidenced by the inertial defect which is approximately −3 u Å^2 for both heterodimers as expected for the methyl group alone. Planarity is also fully supported by the *ab initio* calculations where no symmetry restrictions were imposed and no imaginary frequencies were found as well as by the RAM fitting program where no out-of-plane terms were necessary to fit the spectra. In addition, we made the usual assumption that the structure of the monomers is unchanged on complex formation. So assuming planarity of the heavy atoms and fixing the structures of the monomers, we have three structural parameters to be determined for each heterodimer under consideration. For the CH_3OH–H_2CO heterodimer, we varied the r (O–H), $\theta = \angle$CO–H, and $\phi = \angle$O–HO parameters, and for the CH_3OH–CO_2 heterodimer, we varied the r (C–O), $\theta = \angle$OC–O, and $\phi = \angle$C–OC parameters.

Since the latest available experimental structure for methanol was the r_S structure determined by Gerry et al. [24] in 1976, we decided to make a separate structural fit to determine the r_0 structure of methanol. In this fit, we have used the moments of inertia for the following methanol isotopologues: $^{12}CH_3{}^{16}OH$ [17], $^{12}CD_3{}^{16}OH$ [18], $^{12}CH_3{}^{18}OH$ [25], $^{13}CH_3{}^{16}OH$ [26], $^{12}CH_3{}^{16}OD$ [27], $^{12}CD_3{}^{16}OD$ [28]. The principal axis moments of inertia needed for the structural fit were obtained from diagonalization of the rho-axis moment of inertia tensors, which were determined for the methanol isotopologues listed above from Refs. [17,18,25–28]. A conversion factor 505379.01 MHz u Å^2 was used. As initial values for the structural parameters of methanol, we took the parameters of the r_S structure from Gerry et al. [24]. A least-squares fit to I_a, I_b, and I_c of the six methanol isotopologues mentioned above showed that the value of the tilt angle (the angle between CO bond and symmetry axis of the methyl group) is not determined (the value was about 0.1° whereas uncertainty was about 2°). Fixing the tilt angle at zero gave almost the same root-mean-square (rms) deviation for the principal moments of inertia and, therefore, we adopted the structure fit with tilt angle fixed at zero (the rms deviation from the structural fit of the principal moments of inertia was 0.0089 u Å^2). The resulting r_0 structural parameters obtained for methanol are given in Table 3. These parameters were fixed in the structural fits of the heterodimers under consideration. For formaldehyde, the r_0 geometry used is r_0 (CH) = 1.106(1) Å, r_0 (CO) = 1.2067(5) Å, and $\angle$HCO = 121.6(1)° from least-squares fit to I_a and I_b for seven isotopic forms [29–31] with a rms deviation of 0.0033 u Å^2 for the moments of inertia. For carbon dioxide, the geometry employed is r_0 (CO) = 1.162026(34) Å determined by fitting I_b values for six isotopic forms from ref. [32] with a rms deviation of 0.0032 u Å^2 for the moments of inertia.

Table 3
CH_3OH r_0-structural parameters

Parameter	Experimental value	*Ab initio* MP2/aug-cc-pVTZ
r_{CH} (Å)	1.09217(62)	1.091
r_{OH} (Å)	0.9709(18)	0.961
r_{CO} (Å)	1.42607(46)	1.426
$\angle$HCH(°)	108.735(68)	108.9
$\angle$COH(°)	107.48(17)	108.5

As in the case of methanol, the rigid rotor rotational constants shown in Table 4 were determined from diagonalization of the rho-axis rotational constants obtained in the present study. The structural parameters resulting from the least-squares fits to I_a and I_b moments of inertia of isotopologues of CH_3OH–CO_2 and CH_3OH–H_2CO heterodimers are presented in Table 5 and Figs. 3 and 4, respectively. The rms deviation from the structural fit to I_a and I_b moments of inertia was 0.055 u Å^2 for CH_3OH–H_2CO, CH_3OH–D_2CO and CH_3OH–$H_2{}^{13}CO$ isotopologues of CH_3OH–H_2CO heterodimer and 0.039 u Å^2 for CH_3OH–CO_2, CD_3OH–CO_2, and CH_3OH–$^{13}CO_2$ isotopologues of CH_3OH–CO_2 heterodimer. It should be noted that structural fits with the I_c moments included gave differences in structural parameters within the 1σ uncertainties for CH_3OH–H_2CO heterodimer and within the combined 2σ uncertainties for the CH_3OH–CO_2 heterodimer. However, for both heterodimers, the rms deviations of the fits increased by a factor of ≈4. Therefore, we decided to omit the I_c moments of inertia from the final fits, since in our view, they are contaminated by the effects of librational motions more than I_a and I_b moments of inertia.

Table 4
Rigid-rotor rotational constants for isotopic forms of CH_3OH–H_2CO and CH_3OH–CO_2

Isotopic species	A (MHz)	B (MHz)	C (MHz)
CH_3OH–CO_2	9456.807	2464.270	1976.439
CH_3OH–$^{13}CO_2$	9453.557	2443.447	1962.905
CD_3OH–CO_2	8921.632	2228.243	1824.864
CH_3OH–H_2CO	27315.981	2374.422	2219.302
CH_3OH–$H_2{}^{13}CO$	27001.674	2329.984	2178.632
CH_3OH–D_2CO	24418.402	2258.944	2098.717

Table 5
CH_3OH–H_2CO and CH_3OH–CO_2 r_0-structural parameters

Species	Parameter	Experimental value	*Ab initio*
CH_3OH–CO_2			
	r_{C-O}(Å)	2.834(3)	2.713[a]/2.75[b]
	∠CO–C(°)	114.4(3)	118.2[a]
	∠O–CO(°)	85.4(1)	94.3[a]
CH_3OH–H_2CO			
	r_{O-H}(Å)	2.097(6)	1.98[c]
	∠CO–H(°)	98.4(3)	108.0[c]
	∠O–HO(°)	140.3(5)	158.2[c]

[a] Present work, MP2/aug-cc-pVTZ.
[b] Klotz et al. [8] employing a B3LYP/6-311++G basis.
[c] Brume et al. [9] using a B3PW91/aug-cc-pVTZ basis.

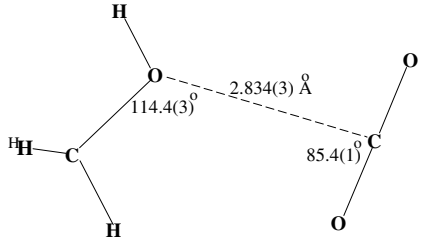

Fig. 3. Structure of CH_3OH–CO_2.

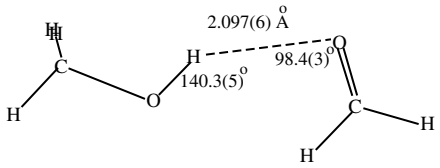

Fig. 4. Structure of CH_3OH–H_2CO.

5. Stark effect measurements

One of the NIST spectrometers is equipped with parallel plates of dimensions 25 cm × 25 cm and about 25 cm spacing. These are placed along the cavity axis centered between the mirrors and the nozzle and located perpendicular to the cavity axis. Positive voltage is applied to one plate and an equal negative voltage is applied to the second plate to obtain Stark effect shifts in the transitions. The microwave electric field and external electric field are parallel so that $\Delta M = 0$ transitions are observed. The Stark plate separation, d, was determined by a calibration with OCS $J = 1$–0 and the known dipole moment of $\mu = 2.3856(10) \times 10^{-30}$ cm [0.71519(3) D] [33].

For the CH_3OH–CO_2 complex, the $M = 0$ and 1 components of the $2_{1,2}$–$1_{0,1}$ transition and the $M = 0$, 1, and 2 components of the $3_{0,3}$–$2_{0,2}$ transition of the A state were measured with applied voltages up to 7 kV (±3.5 kV) with frequency shifts up to 0.9 MHz. For the CH_3OH–H_2CO complex, the $M = 0$, 1, and 2 components of the $3_{1,3}$–$2_{1,2}$ and $3_{1,2}$–$2_{1,1}$ transitions of the A state were measured with voltages up to 12 kV (±6 kV) and maximum shift up to 1.1 MHz. The Stark shifts were least-squares fit to the standard second order asymmetric rotor coefficients of $(\mu_a E/d)^2$ and $(\mu_a E/d)^2$ to derive the μ_a and μ_b dipole moment components listed in Table 6.

6. Discussion

The structural parameters determined experimentally for CH_3OH–CO_2 and CH_3OH–H_2CO are compared to *ab initio* values in Table 5. For CH_3OH–CO_2, we employed a MP2/aug-cc-pVTZ basis set using GAUSSIAN03 [34]. All vibrational frequencies were positive confirming the ground state is a true minimum and one negative frequency was found when the methyl group was rotated by 180° to the saddle point region at the top of the torsional barrier. The methanol–carbon dioxide complex shows a van der Waals bond between its oxygen atom and the carbon atom of CO_2. While the *ab initio* structure is in general agreement with the experimental geometry, the van der Waals bond distance is shorter by nearly 7% and the angles are larger by 10% or more. The barrier to internal rotation of the

Table 6
Comparison of experimental molecular parameters for CH_3OH–CO_2 and CH_3OH–H_2CO with the theoretical values

Parameter	CH_3OH–CO_2 Experiment	Theory MP2/aug-cc-pVTZ	CH_3OH–H_2CO Experiment	Theory[a] B3PW91/aug-cc-pVTZ
A [MHz]	9456.807	9445.9	27315.981	27546.1
B [MHz]	2464.270	2563.7	2374.422	2310.4
C [MHz]	1976.439	2042.4	2219.302	2160.7
μ_a [C · m]	$6.344(7)\times10^{-30}$	6.858×10^{-30}	$3.376(13)\times10^{-30}$	6.71×10^{-30}
μ_a [D]	1.912(2)	2.056	1.012(4)	2.01
μ_b [C · m]	$0.14(1)\times10^{-30}$	1.35×10^{-30}	$2.18(5)\times10^{-30}$	1.17×10^{-30}
μ_b [D]	0.039(3)	0.405	0.655(16)	0.35
μ_T [C · m]	$6.34(1)\times10^{-30}$	7.00×10^{-30}	$4.02(4)\times10^{-30}$	6.80×10^{-30}
μ_T [D]	1.912(3)	2.10	1.205(12)	2.04
CH_3 to a,b-axes				
θ_a [°][b]	47.3/46.3	43.4	24.1/23.2	31.6
θ_b [°][b]	42.7/43.7	46.6	65.9/66.8	58.4

[a] Ref. [9].
[b] The first experimental value is from the structure coordinates and the second value is from the internal rotation parameters.

methyl group is calculated to be 388 cm^{-1} while the experimental value is 175 cm^{-1}. The poor agreement demonstrates the difficulty *ab initio* methods have in determining the structures and other properties of complexes with broad and shallow potential wells. The experimental structure of CH_3OH–H_2CO is compared with the theoretical results reported by Bruner et al. [9]. Very similar offsets in the H-bond distances and angles between theory and experiment are seen there as well.

Further comparisons of the theoretical and experimental values of the rotational constants, dipole moments, and methyl symmetry axis angles relative to the a and b principal axes, θ_a and θ_b, are given in Table 6. These angles can be derived from the structure coordinates or from the internal rotation parameters. Generally, good agreement was obtained for all parameters except for the dipole moment components μ_b for CH_3OH–CO_2 and μ_a for CH_3OH–H_2CO. While the theoretical values deviate to a larger extent than is typical for calculations of the monomer properties, they are in reasonable agreement with the structures employed in the methanol–carbon dioxide ice studies [5–8] and in the reaction coordinate study of dihydrogen exchange for methanol–formaldehyde [9].

7. Summary

We have observed the microwave spectra of several isotopologues for the CH_3OH–CO_2 and CH_3OH–H_2CO heterodimers with a pulsed-beam FTMW spectrometer. Both complexes show spectra of the A and E torsional states arising from the methyl group internal rotation. Stark effect measurements permitted the determination of the electric dipole moment components. The moments of inertia for three isotopic forms of each heterodimer were fit to three structural parameters; an intermolecular bond distance and two angles between the monomers. The experimental molecular parameters have been compared to theoretical values where available.

Acknowledgment

The authors would like to thank Dr. I. Kleiner for making her global fitting program available for this work.

Appendix A. Supplementary data

Supplementary data for this article are available on ScienceDirect (www.sciencedirect.com) and as part of the Ohio State University Molecular Spectroscopy Archives (http://msa.lib.ohio-state.edu/jmsa_hp.htm).

References

[1] C.W. Gillis, J.Z. Gillis, R.D. Suenram, F.J. Lovas, E. Kraka, D. Cremer, J. Am. Chem. Soc. 113 (1991) 2412–2421.
[2] F.J. Lovas, H. Hartwig, J. Mol. Spectrosc. 183 (1997) 98–109.
[3] C.L. Lugez, F.J. Lovas, J.T. Hougen, N. Ohashi, J. Mol. Spectrosc. 194 (1999) 95–112.
[4] F.J. Lovas, R.D. Suenram, L.H. Coudert, J. Chem. Phys. 92 (1990) 891–898.
[5] P. Ehrenfreund, E. Dartois, K. Demyk, L. D'Hendecourt, Astron. Astrophys. 339 (1998) L17–L20.
[6] P. Ehrenfreund, O. Kerkhof, W.A. Schutte, A.C.A. Boogert, P.A. Gerakines, E. Dartois, L. D'Hendecourt, A.G.G.M. Tielens, E.F. van Dishoeck, D.C.B. Whittet, Astron. Astrophys. 350 (1999) 240–253.
[7] E. Dartois, K. Demyk, L. D'Hendecourt, P. Ehrenfreund, Astron. Astrophys. 351 (1999) 1066–1074.
[8] A. Klotz, T. Ward, E. Dartois, Astron. Astrophys. 416 (2004) 801–810.
[9] Y. Brumer, M. Shapiro, P. Brumer, K.K. Baldridge, J. Phys. Chem. A 106 (2002) 9512–9519.
[10] F.J. Lovas, R.D. Suenram, J. Chem. Phys. 87 (1987) 2010–2020.
[11] R.D. Suenram, F.J. Lovas, G.T. Fraser, J.Z. Gillies, C.W. Gillies, M. Onda, J. Mol. Spectrosc. 137 (1989) 127–137.
[12] T.J. Balle, W. Flygare, Rev. Sci. Instrum. 52 (1981) 33–45.
[13] J.-U. Grabow, private communication (2003); see www.pci.unihannover.de/~lgpca/spectroscopy/ftmw/.
[14] B.N. Taylor, C.E. Kuyatt, NIST Tech. Note 1297 (1994). The publication may be downloaded from http://physics.nist.gov/Pubs/guidelines/contents.html.
[15] (a) W.A. Majewski, J.F. Pfanstiel, D.F. PLusquellic, D.W. Pratt, in: A.B. Myers, T.R. Rizzo (Eds.), Laser Techniques in Chemistry, Vol. XXIII, Wiley, New York, 1995, pp. 101–148;

(b) D.F. Plusquellic, R.D. Suenram, B. Mate, J.O. Jensen, A.C. Samuels, J. Chem. Phys. 115 (2001) 3057–3067.
[16] J.T. Hougen, I. Kleiner, M. Godefroid, J. Mol. Spectrosc. 163 (1994) 559–586.
[17] L-H. Xu, J.T. Hougen, J. Mol. Spectrosc. 173 (1995) 540–551.
[18] M. Walsh, L.-H. Xu, R. Lees, J. Mol. Spectrosc. 187 (1998) 85–93.
[19] C.C. Lin, J.D. Swalen, Rev. Mod. Phys. 31 (1959) 841–891.
[20] F.J. Lovas, C.L. Lugez, J. Mol. Spectrosc. 179 (1996) 320–323.
[21] G.T. Fraser, F.J. Lovas, R.D. Suenram, J. Mol. Spectrosc. 167 (1994) 231–235.
[22] H.B. Thompson, J. Chem. Phys. 47 (1967) 3407–3410.
[23] R.H. Schwendeman, in: D.R. LideJr., M.A. Paul (Eds.), Critical Evaluation of Chemical and Physical Structural Information, National Academy of Sciences-National Research Council, Washington, DC, 1974, pp. 94–115.
[24] M.C.L. Gerry, R.M. Lees, G. Winnewisser, J. Mol. Spectrosc. 61 (1976) 231–242.
[25] M. Ikeda, Y.-B. Duan, S. Tsunekawa, K. Takagi, The Astrophysical Journal Supplememnt Series 117 (1998) 249–259.
[26] L.-H. Xu, M. Walsh, R. Lees, J. Mol. Spectrosc. 179 (1996) 269–281.
[27] M.S. Walsh, L.-H. Xu, R.M. Lees, I. Mukhopadhyay, G. Moruzzi, B.P. Winnewisser, S. Albert, R.A.H. Batler, F.C. DeLucia, J. Mol. Spectrosc. 204 (2000) 60–71.
[28] L.H. Xu, H.S.P. Müller, F.F.S. van der Tak, S. Thorwirth, J. Mol. Spectrosc. 228 (2004) 220–229.
[29] R. Cornet, G. Winnewisser, J. Mol. Spectrosc. 80 (1980) 438–452.
[30] R. Cornet, B.M. Landsberg, G. Winnewisser, J. Mol. Spectrosc. 82 (1980) 253–263.
[31] R. Bocquet, J. Demaison, J. Cosléou, A. Friedrick, L. Margules, S. Macholl, H. Mäder, M.M. Beaky, G. Winnewisser, J. Mol. Spectrosc. 195 (1999) 345–355.
[32] G. Graner, C. Rossetti, D. Bailly, Mol. Phys. 58 (1986) 627–636.
[33] J.M.L.J. Reinhartz, A. Dymanus, Chem. Phys. Lett. 24 (1974) 346–351.
[34] M. J. Frisch, G. W. Trucks, H. B. Schlegel, G. E. Scuseria, M. A. Robb, J. R. Cheeseman, J. A. Montgomery, Jr., T. Vreven, K. N. Kudin, J. C. Burant, J. M. Millam, S. S. Iyengar, J. Tomasi, V. Barone, B. Mennucci, M. Cossi, G. Scalmani, N. Rega, G. A. Petersson, H. Nakatsuji, M. Hada, M. Ehara, K. Toyota, R. Fukuda, J. Hasegawa, M. Ishida, T. Nakajima, Y. Honda, O. Kitao, H. Nakai, M. Klene, X. Li, J. E. Knox, H. P. Hratchian, J. B. Cross, C. Adamo, J. Jaramillo, R. Gomperts, R. E. Stratmann, O. Yazyev, A. J. Austin, R. Cammi, C. Pomelli, J. W. Ochterski, P. Y. Ayala, K. Morokuma, G. A. Voth, P. Salvador, J. J. Dannenberg, V. G. Zakrzewski, S. Dapprich, A. D. Daniels, M. C. Strain, O. Farkas, D. K. Malick, A. D. Rabuck, K. Raghavachari, J. B. Foresman, J. V. Ortiz, Q. Cui, A. G. Baboul, S. Clifford, J. Cioslowski, B. B. Stefanov, G. Liu, A. Liashenko, P. Piskorz, I. Komaromi, R. L. Martin, D. J. Fox, T. Keith, M. A. Al-Laham, C. Y. Peng, A. Nanayakkara, M. Challacombe, P. M. W. Gill, B. Johnson, W. Chen, M. W. Wong, C. Gonzalez, J. A. Pople, GAUSSIAN03, Revision B.04, Gaussian Inc., Pittsburgh, PA, 2003.